J|A|C|S COMMUNICATIONS

Published on Web 04/14/2010

A Xenon-Based Molecular Sensor Assembled on an MS2 Viral Capsid Scaffold

Tyler Meldrum, Kristen L. Seim, Vikram S. Bajaj, Krishnan K. Palaniappan, Wesley Wu, Matthew B. Francis, David E. Wemmer, and Alexander Pines*

College of Chemistry, University of California, Berkeley, Berkeley, California 94720 and Lawrence Berkeley National Laboratory, Materials Sciences Division and Physical Biosciences Division, Berkeley, California 94720

Received January 13, 2010; E-mail: pines@berkeley.edu

The refinement of targeted contrast agents is crucial for progress in molecular imaging. The primary contrast agents in use in magnetic resonance imaging (MRI) either modulate magnetic relaxation (e.g., gadolinium-based contrast agents[1]) or reduce bulk magnetization via exchange of saturated nuclei from a magnetically distinct site (e.g., chemical exchange saturation transfer, or CEST, agents[2,3]). While most contrast agents exploit strong proton signals from abundant water and fat, there are advantages to using exogenous nuclei. In particular, xenon is inert, relaxes slowly, can be reversibly dissolved in solution, and is amenable to hyperpolarization by optical pumping.[4−6] In this work, we present the development of an engineered nanoparticle that combines xenon-based molecular sensors with MS2 viral capsids, conferring dramatically increased solubility and CEST sensitivity to these contrast agents. Furthermore, previous reports have shown that MS2 viral capsids endowed with nucleotide aptamers[7] bind to specific cell receptors and are taken up by the cell, indicating probable biocompatibility. Because each capsid can be targeted to a molecule of interest, the incorporation of multiple sensor units into each individual capsid could facilitate the detection of chemical targets at much lower concentrations than is possible using sensors without the capsid scaffold.

The MS2 viral capsid, composed of 180 monomers, is a porous, nearly spherical structure with icosahedral symmetry. After expression in *E. coli*, the coat protein monomers spontaneously assemble into genome-free, noninfectious capsids. The 32 pores in MS2, each ∼2 nm wide, facilitate access to the interior without disassembly of the capsid. The interior and exterior surfaces of the capsid can be independently modified, both to a high degree, enabling the simultaneous integration of many contrast agent molecules in the interior and cell-specific targeting units on the exterior.[7−11]

Scheme 1. Synthesis of MS2CA Sensors

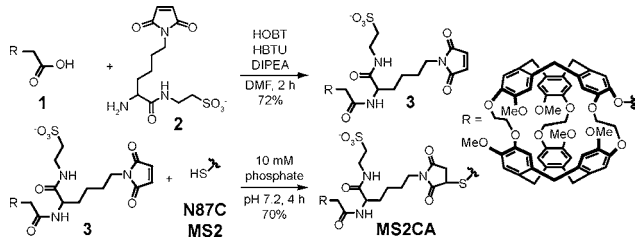

The synthesis of an MS2 capsid scaffold for xenon MRI, shown in Scheme 1, relies on attachment of a xenon-host molecule, the cryptophane-A cage conjugated with acetate as a chemical handle (**1**), to the interior of an MS2 viral capsid. The technique used to attach hydrophobic cryptophane-A to the interior of MS2 has been previously used to attach taxol,[12] another water-insoluble molecule. Attachment requires both a mutation (N87C) in MS2, introducing a solvent-accessible cysteine on the interior of the capsid, and a linker molecule (**2**). The linker contains a maleimide to react selectively with the interior cysteine, a taurine to increase the aqueous solubility of cryptophane-A, and an amine to react with cryptophane-A. (See Supporting Information for complete synthetic protocols and characterization data.) The purified cage-linker (**3**) was reacted with N87C MS2 for 4 h at room temperature in 10 mM phosphate buffer at pH 7.2 to produce the MS2-cage construct, MS2CA. Following purification by size-exclusion chromatography, which confirmed that the viral capsids were fully assembled, MS2CA was membrane-filter concentrated and quantified using SDS-PAGE and optical densitometry. For analysis, ESI-MS was used to confirm that the cage had been attached to the viral capsid and to estimate the extent of modification; approximately 70% conversion was achieved, corresponding to ∼125 copies of cage per capsid.

The ^{129}Xe NMR spectrum of 1 μM cryptophane-A showed a clear peak from xenon dissolved in water (Xe_{aq}) at ∼190 ppm, consistent with previous observations.[13] However, no signal corresponding to xenon in the cryptophane cage (Xe@cage) was observed directly. Consequently, we employed the Hyper-CEST detection method.[14,15] By applying a selective-bandwidth saturation pulse and monitoring saturation transfer to the Xe_{aq} peak, we observed the presence of a Xe@cage peak at ∼60 ppm. Details of the frequency-selective saturation sequences and other experimental parameters used in these experiments are provided as Supporting Information.

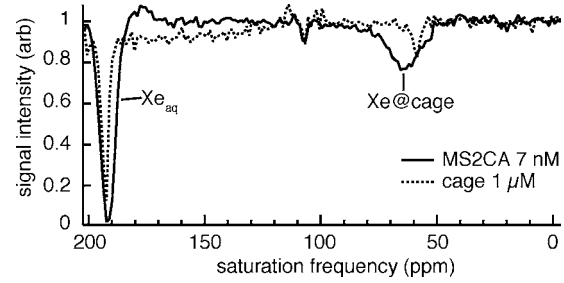

Figure 1. Saturation transfer spectra of the cage and MS2CA systems. The peaks at ∼190 ppm correspond to Xe_{aq}, while those at ∼60 ppm are Xe@cage. The feature at ∼110 ppm is anomalous.

To compare the performance of the MS2CA sensor with that of the unconjugated cage, we measured magnetization transfer in 7 nM MS2CA (assembled MS2CA units, corresponding to 1 μM coat protein monomers) and 1 μM cage solutions by incrementally varying the frequency of the applied saturation pulse. These spectra are shown in Figure 1. The contrast was comparable for both solutions. We note a downfield shift of the Xe@cage peak and a

 10.1021/ja100319f

slight upfield shift of the Xe_{aq} peak in the MS2CA spectrum. Furthermore, we observe significant broadening of the Xe@cage saturation peak, from ~1 kHz in the cage-only system to ~5 kHz in MS2CA. Achieving a strong Hyper-CEST effect in spite of line broadening of the Xe@cage in MS2CA is still possible by using saturation pulses with intentionally large bandwidths.

To determine the detection threshold for MS2CA, we investigated dilutions of MS2CA to 700, 70, 7, and 0.7 pM (assembled capsids), as well as a control solution containing 10 mM phosphate buffer. For each sample, we collected saturation profiles by employing saturation pulses at the Xe@cage frequency for incremental saturation times. Three of these trials are summarized in Figure 2. Magnetization transfer was apparent in all MS2CA cases; the 0.7 pM MS2CA represents the lowest concentration of detected xenon-based molecular sensors to date. The increased sensitivity over a measurement of 10 nM cryptophane-A reported by Schröder et al.[16] is due both to the incorporation of ~125 cages per MS2CA molecule and to various technical improvements,[17] including enhanced saturation transfer methods applicable to systems with broad NMR lines.[18]

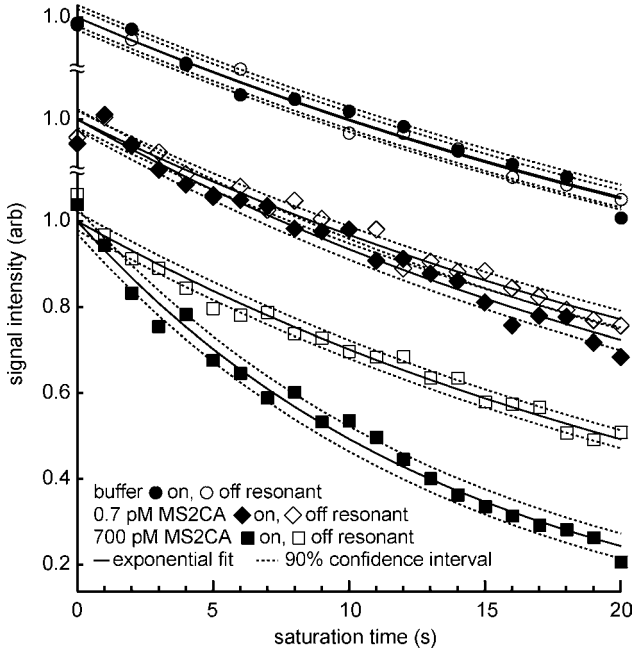

Figure 2. Saturation profiles of the buffer (top), 0.7 pM MS2CA (middle), and 700 pM MS2CA (bottom) solutions. After 20 s of saturation, contrast between the off and on resonance saturation experiments is evident in the MS2CA cases, indicating the presence of contrast agent. None of the experiments is corrected for relaxation, hence the decay in signal intensity in the off resonant saturation profiles. Exponential fits are given as solid lines. The three data sets are vertically offset for visibility.

The incorporation of many xenon hosts into the MS2 viral capsid scaffold significantly lowers the detection threshold of binding targets and improves the solubility and potential biocompatibility of an otherwise hydrophobic host molecule. Although this is not the first application of a scaffold to produce an amplified molecular sensor,[19] it has many more sensor molecules per targeting unit and demonstrates greater sensitivity than many previous multivalent scaffolds. While some multivalent gadolinium-based scaffolds produce greater contrast in ^{1}H MRI studies, there is growing concern over the in vivo toxicity of such contrast agents.[20] Additionally, other contrast mechanisms that rely on enzymes[21] or zeolites[22] show potential as sensitive molecular sensors. However, both of these methods rely on direct detection of xenon, requiring both high concentration and polarization of ^{129}Xe in the sample.

We are currently exploring the influence of solvent exposure on the kinetics of both xenon exchange and saturation, properties that may be affected by the geometry of the MS2 capsid and that could improve saturation transfer-based detection techniques. In addition, one could further increase detection sensitivity of these molecular sensors by physical extraction of xenon through a phase change,[23] by increasing the isotopic abundance of ^{129}Xe, or by increasing the xenon polarization.[24] We anticipate that a combination of these techniques will eventually permit detection of targets at femtomolar concentrations, finding application in portable analytical devices and greatly enhancing sensitivity for in vivo analytes.

Acknowledgment. This work was supported by the Director, Office of Science, Office of Basic Energy Sciences, Materials Sciences and Engineering Division, of the U.S. Department of Energy under Contract Nos. DE-AC03-76SF00098 and DE-AC02-05CH11231.

Supporting Information Available: Synthetic protocols and characterization of MS2CA constructs, saturation pulse and other experimental parameters, saturation profiles for all MS2CA solutions. This material is available free of charge via the Internet at http://pubs.acs.org.

References

(1) Hendrick, R. E.; Haacke, E. M. *J. Magn. Reson. Imaging* **1993**, *3*, 137–148.
(2) Sherry, A. D.; Woods, M. *Annu. Rev. Biomed. Eng.* **2008**, *10*, 391–411.
(3) Zhang, S.; Merritt, M.; Woessner, D.; Lenkinski, R. E.; Sherry, A. *Acc. Chem. Res.* **2003**, *36*, 783–790.
(4) Berthault, P.; Huber, G.; Desvaux, H. *Prog. Nucl. Magn. Reson. Spectrosc.* **2009**, *55*, 35–60.
(5) Goodson, B. *J. Magn. Reson.* **2002**, *155*, 157–216.
(6) Seward, G. K.; Wei, Q.; Dmochowski, I. J. *Bioconjugate Chem.* **2008**, *19*, 2129–2135.
(7) Tong, G. J.; Hsiao, S. C.; Carrico, Z. M.; Francis, M. B. *J. Am. Chem. Soc.* **2009**, *131*, 11174–11178.
(8) Allen, M.; Bulte, J.; Liepold, L.; Basu, G.; Zywicke, H.; Frank, J.; Young, M.; Douglas, T. *Magn. Reson. Med.* **2005**, *54*, 807–812.
(9) Datta, A.; Hooker, J.; Botta, M.; Francis, M.; Aime, S.; Raymond, K. *J. Am. Chem. Soc.* **2008**, *130*, 2546–2552.
(10) Hooker, J. M.; Datta, A.; Botta, M.; Raymond, K. N.; Francis, M. B. *Nano Lett.* **2007**, *7*, 2207–2210.
(11) Prasuhn, D., Jr.; Yeh, R.; Obenaus, A.; Manchester, M.; Finn, M. *Chem. Commun.* **2007**, 1269–1271.
(12) Wu, W.; Hsaio, S. C.; Carrico, Z. M.; Francis, M. B. *Angew. Chem., Int. Ed.* **2009**, *48*, 9493–9497.
(13) Spence, M. M.; Rubin, S. M.; Dimitrov, I. E.; Ruiz, E. J.; Wemmer, D. E.; Pines, A. *Proc. Natl. Acad. Sci. U.S.A.* **2001**, *98*, 10654–10657.
(14) Schröder, L.; Lowery, T.; Hilty, C.; Wemmer, D.; Pines, A. *Science* **2006**, *314*, 446–449.
(15) Ruppert, K.; Brookeman, J. R.; Hagspiel, K. D.; Mugler, J. P. I. *Magn. Reson. Med.* **2000**, *44*, 349–357.
(16) Schröder, L.; Meldrum, T.; Smith, M.; Lowery, T.; Wemmer, D.; Pines, A. *Phys. Rev. Lett.* **2008**, *100*, 257603(4).
(17) Refinements to the xenon delivery system plus an increase of the xenon gas concentration from 1% to 2% have reduced shot noise and increased signal considerably.
(18) Bajaj, V. S.; Meldrum, T.; Wemmer, D. E.; Pines, A. *J. Magn. Reson.* **2010**, in press.
(19) Mynar, J. L.; Lowery, T. J.; Wemmer, D. E.; Pines, A.; Fréchet, J. M. J. *J. Am. Chem. Soc.* **2006**, *128*, 6334–6335.
(20) Ersoy, H.; Rybicki, F. J. *J. Magn. Reson. Imaging* **2007**, *26*, 1190–1197.
(21) Wei, Q.; Seward, G.; Hill, P.; Patton, B.; Dimitrov, I.; Kuzma, N.; Dmochowski, I. *J. Am. Chem. Soc.* **2006**, *9*, 13274–13283.
(22) Lerouge, F.; Melnyk, O.; Durand, J.; Raehm, L.; Berthault, P.; Huber, G.; Desvaux, H.; Constantinesco, A.; Choquet, P.; Detour, J. *J. Mater. Chem.* **2009**, *19*, 379–386.
(23) Zhou, X.; Graziani, D.; Pines, A. *Proc. Natl. Acad. Sci. U.S.A.* **2009**, *106*, 16903–16906.
(24) Schrank, G.; Ma, Z.; Schoeck, A.; Saam, B. *Phys. Rev. A* **2009**, *80*, 063424(10).

JA100319F